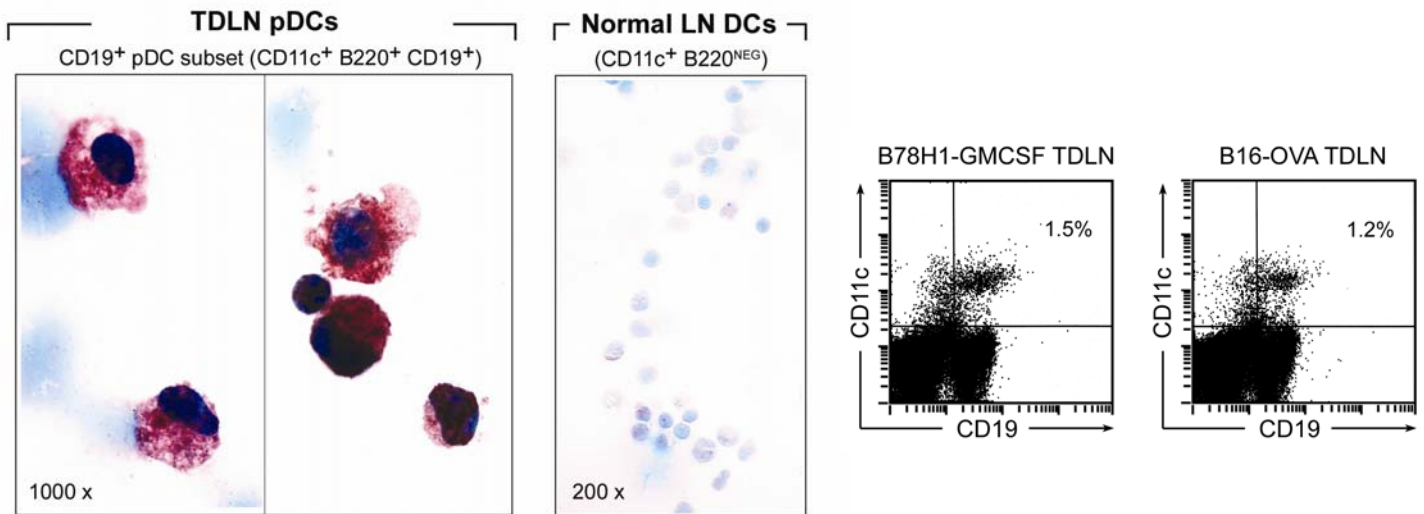


Supplemental Data



	B78H1-GMCSF	B16-OVA
Total cells/TDLN (millions)	4.2, 4.3, 4.0	3.6, 3.2, 3.4
Absolute CD19 ⁺ pDCs / LN (CD19 ⁺ B220 ⁺ CD11c ⁺) (thousands)	40, 49, 55	18, 15, 37
mean±SD CD19 ⁺ pDCs / LN (thousands)	48 ± 7	23 ± 11

Figure S1. IDO expression by the CD19⁺ cells in the pDC fraction of TDLNs.

(Left) IDO staining (red color) of cytocentrifuge preparations of sorted CD19⁺ pDCs (CD11c⁺B220⁺CD19⁺ cells) from TDLNs of B78H1-GMCSF tumors. We have previously shown that this CD19⁺ subset of pDCs contains essentially all of the functional IDO-mediated suppressor activity in these TDLNs (1). Control cells (the non-plasmacytoid DC fraction of normal LNs) showed minimal IDO staining. Staining controls (neutralization of the primary antibody with an excess of the immunizing peptide) were all negative, as previously described (2). **(Right)** FACS plots of gated B220⁺ cells from TDLNs, showing the CD11c⁺ CD19⁺ subset (the CD19⁺ pDCs sorted at left). **(Table)** Quantitatively, the B78H1-GMCSF tumors yielded about twice as many CD19⁺ pDCs as the B16-OVA tumors, as shown in the table.

The CD19⁺ subset of pDCs typically comprised 30-50% of total pDCs in TDLNs. Because the number of CD19⁺ pDCs was so small, their viability was improved if they were sorted as part of the total pDC fraction (CD11c⁺ B220⁺). Therefore, this was the preparation routinely used as the source of IDO-expressing cells for functional assays, as in our previous reports (1, 3). Since the effects of IDO were dominant, it was immaterial whether other IDO^{NEG} pDCs were also present in the assays.

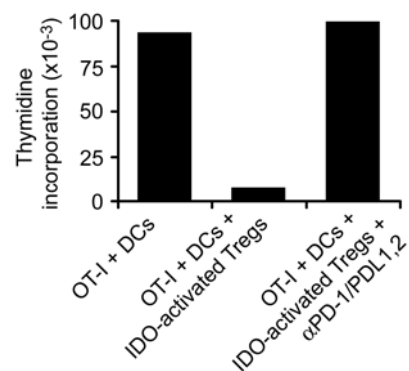


Figure S2. IDO-activated Tregs can suppress CD8⁺ T cells.

Tregs were activated for 2 days in co-culture with TDLN pDCs+OT-I cells+OVA peptide (pre-activation cultures, as described in manuscript Figure 2). Activated Tregs were harvested, re-sorted, and added to readout assays comprising CD8⁺ OT-I T cells + CD11c splenic DCs from B6 mice + OVA peptide.

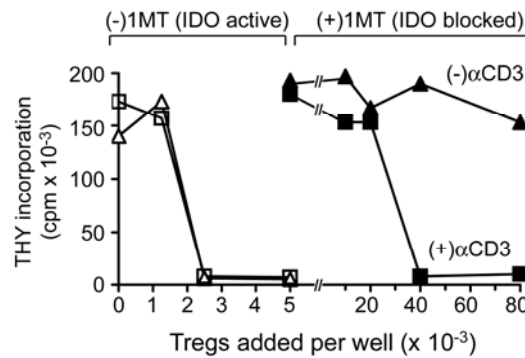


Figure S3. Tregs mediate suppression of bystander A1 cells in mixed co-cultures.

A1 T cells and CBA DCs were added directly to the Treg pre-activation assay at the start of culture. (Thus, the combined cultures comprised IDO⁺ pDCs, OT-I T cells, Tregs, A1 T cells, CBA splenic DCs, and feeder layer.) This approach does not distinguish which population(s) of T cells were proliferating, nor was it designed to distinguish direct suppression (mediated by the IDO itself, e.g., via soluble tryptophan metabolites) from suppression mediated by the IDO-activated Tregs. However, the mixed co-cultures addressed the specific question of whether IDO and activated Tregs could produce effective levels of suppression rapidly enough that they could suppress the bystander A1 cells before they could begin dividing.

A titration of Tregs was added to the mixed co-culture assays described above, either with IDO active (no 1MT added), or with IDO blocked by 1MT, as shown. In each case, parallel titrations were performed with or without the addition of αCD3 mAb. (The A1 and OT1 cells were already maximally activated by their respective cognate peptides, and αCD3 showed no further effect on these cells, data not shown; the relevant effect of the αCD3 was thus to activate the Tregs).

In the absence of Tregs there was substantial proliferation of T cells in co-cultures, despite the presence of IDO⁺ pDCs. However, the addition of fewer than 5000 Tregs was sufficient to suppress proliferation of all cells in culture. (Suppression was not further enhanced by αCD3 mAb, indicating that Tregs were already maximally suppressive). In contrast, when IDO was blocked by 1MT, then even 10-fold more Tregs showed no spontaneous suppressor activity in the absence of αCD3 mAb. The addition of αCD3 mAb allowed Tregs to suppress even without active IDO, but suppression was an order of magnitude less effective than when IDO was active.

Thus, the results of the mixed co-culture model were similar to those using the separate pre-activation and re-sorting step.

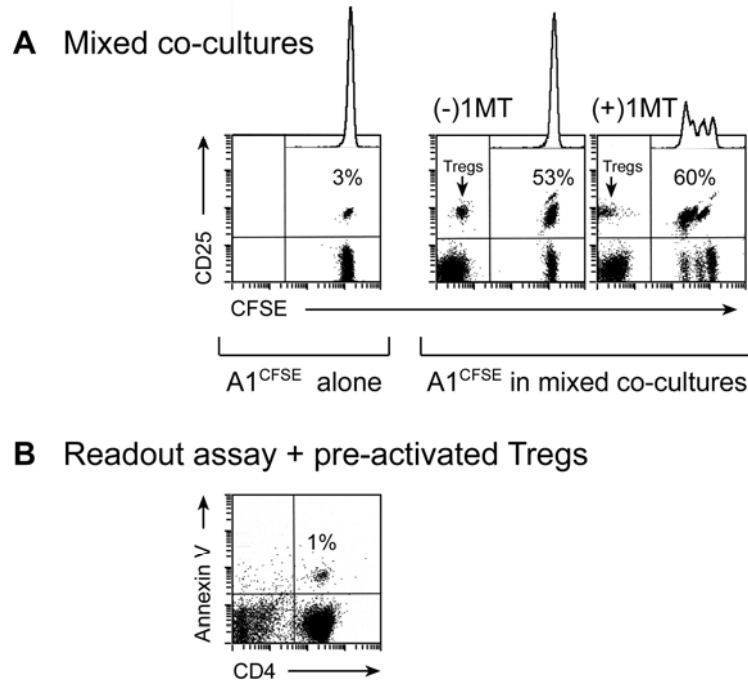


Figure S4. Suppressed A1 cells upregulate activation markers but do not divide.

(A) Mixed co-cultures were established as in Figure S3, comprising Treg activation cultures (IDO⁺ pDCs, OT-I cells, Tregs, and feeder layer) plus the direct addition of CFSE-labeled CD4⁺ sorted A1 T cells + CBA DCs + HY peptide. After 2-3 days the mixed co-cultures were harvested and stained for CD25 vs. CFSE. Percentages show the fraction of A1 cells that were CD25⁺. (Similar results were also obtained with CD44 staining, data not shown.) Without activation, A1^{CFSE} cells were <5% CD25⁺. In co-cultures containing IDO-activated Tregs (without 1MT), the A1^{CFSE} cells showed upregulation of activation markers (CD25 and CD44) on a proportion of cells, but were not able to divide. When IDO was blocked (+1MT) the A1^{CFSE} cells upregulated activation markers and were able to divide.

(B) IDO-activated Tregs were sorted as described in manuscript Figure 2 and added to readout assays of A1 cells + CBA DCs + HY peptide. After 3 days, cells were harvested and stained for CD4 vs. annexin V-PE. Minimal apoptosis of the suppressed A1 cells was observed.

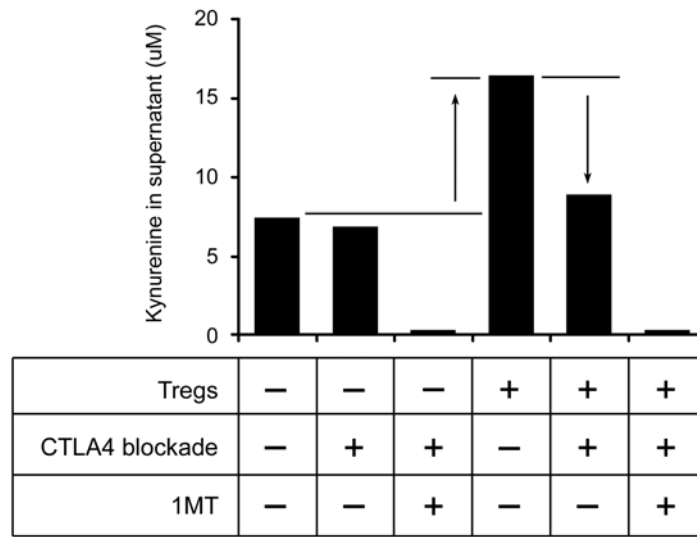


Figure S5. Tregs increase IDO enzymatic activity in a CTLA4-dependent fashion.

TDLN pDCs (1×10^4) and OT1 T cells (1×10^5) were cultured for 3 days, with or without 1×10^4 Tregs. Replicate wells received 10 ug/ml anti-CTLA4-blocking antibody (clone 9H10), and/or 1MT, as shown. After 3 days, the culture supernatants were analyzed by HPLC for the concentration of kynurenine (4). The absolute amount of kynurenine that accumulated in the supernatant was variable, since kynurenine is metabolized to other downstream products, but the relative amounts were informative. The arrows show that the addition of Tregs to the culture increased the production of kynurenine above the basal level produced by the IDO⁺ pDCs and OT-I alone; and that this Treg-induced increase was blocked by anti-CTLA4 mAb. The basal level of IDO, which was fully sufficient to inhibit the proliferation of the OT-I cells, was not blocked by anti-CTLA4 mAb (second bar). Thus, the effect of Tregs was to cause a “super-induction” of IDO, in a CTLA4-dependent fashion.

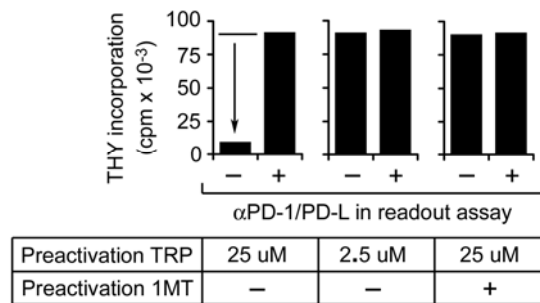


Figure S6. IDO-induced Treg activation cannot be created when the medium contains insufficient tryptophan.

To test the hypothesis that the putative soluble factor responsible for Treg activation might be a metabolite of tryptophan, we asked whether Treg activation would be prevented if the total available of tryptophan in the culture medium was made artificially low. (Because each metabolite is made in a 1:1 stoichiometry, the level of metabolites produced is strictly limited by the initial concentration of tryptophan.) Cultures were set up containing TDLN pDCs + Tregs + OT-I + feeder cells, with normal or low concentrations of tryptophan in the medium. Figure S3 shows that conducting the pre-activation step in 2.5 uM tryptophan (1/10th the usual concentration) completely prevented the pre-activation of Tregs by IDO. This lower level of tryptophan was still ample to fully support proliferation of effector T cells (ref. (1)), so the reduced level of tryptophan itself was not toxic. Thus, the inability of IDO to activate Tregs under conditions of low tryptophan suggested that there might be an obligate role for tryptophan metabolites in IDO-induced Treg activation.

Additional details of methods

Isolation of tumor-draining lymph node DCs

Tumors were initiated using 1×10^6 B78H1·GM-CSF cells, a sub-line of B16 melanoma transfected with GM-CSF, that recruits many DCs into TDLNs (5, 6), a gift of H. Levitsky. This model was used in our previous reports, because it recruits a large number of IDO⁺ pDCs in TDLNs (1, 3). To rule out any effect of the GMCSF transgene, all key findings were also replicated with B16F10 and/or B16F10-OVA, with similar results. The advantage of the GM-CSF-transfected tumor cells was that they yielded more cells from each TDLN, thus reducing the number of mice required. FACS analysis showed that the pDCs recruited by B78H1·GM-CSF tumors were phenotypically identical to those recruited by B16F10 tumors (1).

Tumors were implanted in the thigh of either B6 mice or IDO-KO mice on the B6 background, positioned so as to drain to the inguinal LN as described (1). Inguinal TDLNs were removed for cell sorting on day 11-14. IDO⁺ DCs were enriched using high-speed MoFlo cell-sorting for CD11c⁺ B220⁺ cells as described (1). This fraction included the specific subset of CD19⁺ CD11c⁺ B220⁺ cells that we have shown to comprise virtually all of the IDO-mediated suppression in TDLNs (1). While CD19 is usually considered a marker for B cells, it has been shown that a subset of pDCs also expresses B-lineage markers (7, 8). We have shown that the CD19⁺ “IDO-competent” DC population in spleen mediates IDO-induced suppression in a number of settings (9, 10). The viability and recovery of the IDO⁺ subset was improved during sorting if the CD19⁺ cells were isolated as part of the total pDC fraction (CD11c⁺ B220⁺ cells). In our studies, it was irrelevant whether the IDO⁺ pDCs were strictly purified; it was only necessary that a population of IDO⁺ cells be present. Therefore, we used the total pDC fraction (CD11c⁺ B220⁺) as the source IDO⁺ cells, just as in our previous studies (1, 3, 11).

Feeder layer

Sorted IDO⁺ pDCs required survival factors to maintain viability and function in vitro. As a feeder layer we added T cell-depleted spleen cells (1×10^5 sorted CD4^{NEG} CD8^{NEG} cells) to all assays. This feeder layer was required, but was entirely nonspecific, and could be derived from any host regardless of MHC haplotype (H2^b, H2^k or H2^d), strain background (B6, CBA, Balb/c or 129), or genotype (GCN2-KO, IDO-KO or Foxp3-KO/scurfy mice). The feeder layer could be fully replaced by a cocktail of recombinant cytokines, comprising mouse IFN α (1000 U/ml, PBL Biomedical Laboratories, Piscataway, NJ) + mouse IL-10 (100 ng/ml, R&D Systems) + human TGF- β 1 (cross-reactive with mouse, 10 ng/ml, R&D Systems). When recombinant cytokines were used, Treg activation still required the presence of IDO⁺ pDCs, and was still abrogated by 1MT. Thus, the function of the feeder layer was purely supportive.

FACS staining

Antibodies were from BD-Pharmingen unless otherwise noted. Anti-mouse CD25-APC conjugate (clone PC61, cat. # 17-0251-81) was from eBioscience; we found that this conjugate gave brighter signal and better separation of CD25⁺ cells than other conjugates from other suppliers. For intracellular staining of CHOP, live cells were first blocked for 10 min with mouse Fc Block (BD Pharmingen) in 10% fetal calf serum medium, stained with anti-CD4-FITC for 30 min on ice, washed with PBS, then fixed and permeabilized for 20 min in 250 μ l Cytoperm/Cytofix solution (BD Pharmingen) on ice. All subsequent staining and wash steps were in BD Permwash solution. Fixed cells were stained with 1:100 dilution of monoclonal

anti-gadd153/CHOP (sc-7351, Santa Cruz Biotechnology), washed, and stained with secondary monoclonal rat anti-mouse-IgG1-PE (#550083, BD Biosciences). This secondary antibody was selected because it did not cross-react with surface immunoglobulin on mouse B cells, which was important for staining mouse T cells using a mouse primary antibody. For Foxp3 staining, anti-Foxp3-PE antibody (clone FJK-16s) was obtained from eBioscience and used per the manufacturer's protocol. For Foxp3 staining, assays omitted A1 bystander cells and Tregs were identified by CD4 expression, as for CHOP staining. Biotinylated anti-PD-L1 (clone MIH5) and anti-PD-L2 (clone TY25) were purchased from eBioscience.

DC adoptive transfer

The DC adoptive-transfer model has been previously described (1, 3). Briefly, total CD11c⁺ DCs were sorted from TDLNs, pulsed with SIINFEKL peptide, and 5×10^4 DCs injected subcutaneously into each anteriopmedial thigh of recipient mice. Recipients had been pre-loaded one day before DC injection with 5×10^6 sorted CD8⁺ OT-I cells. After 4 days, the inguinal LNs draining the site of DC injection were removed, and CD4⁺CD25⁺ Tregs were isolated by cell-sorting.

CFSE labeling and T cell adoptive transfer

Mice were implanted with B16-OVA tumors. On day 7-8, sorted CD8⁺ T cells from WT OT-I or from OT-I bred onto the GCN2-KO background, were labeled with CFSE, and 5×10^6 cells injected i.v., as described (3). Mice received either vehicle control, or 1MT at a concentration of 2 mg/ml in drinking water. After 4 days, the TDLNs and contralateral LNs (CLN) were harvested and stained for 1B11 (BD-Pharmingen) vs. CD8.

References

1. Munn, D.H., Sharma, M.D., Hou, D., Baban, B., Lee, J.R., Antonia, S.J., Messina, J.L., Chandler, P., Koni, P.A., and Mellor, A. 2004. Expression of indoleamine 2,3-dioxygenase by plasmacytoid dendritic cells in tumor-draining lymph nodes. *J. Clin. Invest.* **114**:280-290.
2. Munn, D.H., Sharma, M.D., Lee, J.R., Jhaver, K.G., Johnson, T.S., Keskin, D.B., Marshall, B., Chandler, P., Antonia, S.J., Burgess, R., et al. 2002. Potential regulatory function of human dendritic cells expressing indoleamine 2,3-dioxygenase. *Science* **297**:1867-1870.
3. Munn, D.H., Sharma, M.D., Baban, B., Harding, H.P., Zhang, Y., Ron, D., and Mellor, A.L. 2005. GCN2 kinase in T cells mediates proliferative arrest and anergy induction in response to indoleamine 2,3-dioxygenase. *Immunity* **22**:633-642.
4. Munn, D.H., Shafizadeh, E., Attwood, J.T., Bondarev, I., Pashine, A., and Mellor, A.L. 1999. Inhibition of T cell proliferation by macrophage tryptophan catabolism. *J. Exp. Med.* **189**:1363-1372.
5. Huang, A.Y., Golumbek, P., Ahmadzadeh, M., Jaffee, E., Pardoll, D., and Levitsky, H. 1994. Role of bone marrow-derived cells in presenting MHC class I-restricted tumor antigens. *Science* **264**:961-965.

6. Borrello, I., Sotomayor, E.M., Cooke, S., and Levitsky, H.I. 1999. A universal granulocyte-macrophage colony-stimulating factor-producing bystander cell line for use in the formulation of autologous tumor cell-based vaccines. *Hum. Gene Ther.* **10**:1983-1991.
7. Pelayo, R., Hirose, J., Huang, J., Garrett, K.P., Delogu, A., Busslinger, M., and Kincade, P.W. 2005. Derivation of 2 categories of plasmacytoid dendritic cells in murine bone marrow. *Blood* **105**:4407-4415.
8. Corcoran, L., Ferrero, I., Vremec, D., Lucas, K., Waithman, J., O'Keeffe, M., Wu, L., Wilson, A., and Shortman, K. 2003. The lymphoid past of mouse plasmacytoid cells and thymic dendritic cells. *J. Immunol.* **170**:4926-4932.
9. Baban, B., Hansen, A., Chandler, P., Manlapat, A., Bingaman, A., Kahler, D., Munn, D., and Mellor, A. 2005. A minor population of splenic dendritic cells expressing CD19 mediates IDO-dependent T cell suppression via type 1 interferon-signaling following B7 ligation. *Int. Immunol.* **17**:909-919.
10. Mellor, A.L., Baban, B., Chandler, P.R., Manlapat, A., Kahler, D.J., and Munn, D.H. 2005. Cutting Edge: CpG oligonucleotides induce splenic CD19+ dendritic cells to acquire potent indoleamine 2,3-dioxygenase-dependent T cell regulatory functions via IFN type 1 signaling. *J. Immunol.* **175**:5601-5605.
11. Hou, D.Y., Muller, A.J., Sharma, M.D., Duhadaway, J.B., Banerjee, T., Johnson, M., Mellor, A.L., Prendergast, G.C., and Munn, D.H. 2007. Inhibition of IDO in dendritic cells by stereoisomers of 1-methyl-tryptophan correlates with anti-tumor responses. *Cancer Res.* **67**:792-801.